Magn Reson Med Sci 2019; 18; 29–35
doi:10.2463/mrms.mp.2017-0141 Published Online: March 8, 2018

MAJOR PAPER

A Comparison of Black-blood T_2 Mapping Sequences for Carotid Vessel Wall Imaging at 3T: An Assessment of Accuracy and Repeatability

Jianmin Yuan[1*], Andrew J. Patterson[2], Pascal P. R. Ruetten[1], Scott A. Reid[3], Jonathan H. Gillard[1], and Martin J. Graves[1,2]

Purpose: This study is to compare the accuracy of four different black-blood T_2 mapping sequences in carotid vessel wall.

Methods: Four different black-blood T_2 mapping sequences were developed and tested through phantom experiments and 17 healthy volunteers. The four sequences were: 1) double inversion-recovery (DIR) prepared 2D multi-echo spin-echo (MESE); 2) DIR-prepared 2D multi-echo fast spin-echo (MEFSE); 3) improved motion-sensitized driven-equilibrium (iMSDE) prepared 3D FSE and 4) iMSDE prepared 3D fast spoiled gradient echo (FSPGR). The concordance correlation coefficient and Bland–Altman statistics were used to compare the sequences with a gold-standard 2D MESE, without blood suppression in phantom studies. The volunteers were scanned twice to test the repeatability. Mean and standard deviation of vessel wall T_2, signal-to-noise (SNR), the coefficient of variance and interclass coefficient (ICC) of the two scans were compared.

Results: The phantom study demonstrated that T_2 measurements had high concordance with respect to the gold-standard (all r values >0.9). In the volunteer study, the DIR 2D MEFSE had significantly higher T_2 values than the other three sequences ($P < 0.01$). There was no difference in T_2 measurements obtained using the other three sequences ($P > 0.05$). iMSDE 3D FSE had the highest SNR ($P < 0.05$) compared with the other three sequences. The 2D DIR MESE has the highest repeatability (ICC: 0.96, [95% CI: 0.88–0.99]).

Conclusion: Although accurate T_2 measurements can be achieved in phantom by the four sequences, *in vivo* vessel wall T_2 quantification shows significant differences. The *in vivo* images can be influenced by multiple factors including black-blood preparation and acquisition method. Therefore, a careful choice of acquisition methods and analysis of the confounding factors are required for accurate *in vivo* carotid vessel wall T_2 measurements. From the settings in this study, the iMSDE prepared 3D FSE is preferred for the future volunteer/patient scans.

Keywords: *black-blood, carotid vessel wall, T_2 mapping*

Introduction

Carotid atherosclerosis is a diffuse, degenerative disease of the carotid arteries, which can cause acute thromboembolic vascular events including stroke and transient ischaemic attack (TIA), leading to a large number of disabilities and deaths.[1,2] Magnetic Resonance Imaging could be used as a useful non-invasive tool to assess carotid plaque vulnerabilities, with high resolution, excellent soft tissue contrast and ability for multi-plane reconstruction. Previous work has shown that multi-contrast MRI can characterize high risk plaque components.[3–8] Besides the traditional "weighted" images, there are several studies which have performed quantitative measurements of the vessel wall and major plaque components' relaxation times both *in vivo* and *ex vivo*[9–14]

Quantitative MRI allows direct measurement of the MR properties of human tissue, which could be more suitable across different MR systems and multi-centre studies. Among the quantitative values, T_2 has been reported to be statistically different in major plaque components.[10]

[1]Department of Radiology, University of Cambridge, Level 5, Box 218, Addenbrooke's Hospital, Hills Rd., Cambridge CB2 0Q, UK
[2]Department of Radiology, Cambridge University Hospitals NHS Foundation Trust, Cambridge, UK
[3]GE Healthcare, Amersham, UK
*Corresponding author, Phone: +44-0-1223-767834,
E-mail: jianmin.yuan@cantab.net

Received: September 26, 2017 | Accepted: February 7, 2018

Quantitative T_2 mapping has the potential to assist plaque component segmentation and plaque type classification.[9] For instance, Chai et al.[13] used a T_2 mapping sequence for plaque lipid segmentation and showed that the lipid area determined from T_2 maps has an excellent correlation ($R = 0.85$ based on individual slices and $R = 0.83$ based on plaque average) with the area measured from histology as a gold standard. Using the T_2 map segmentation, they also found that despite similar degree of stenosis and only modest difference in carotid plaque volume, the lipid area was significantly higher in symptomatic compared with asymptomatic plaques.[13]

Several pulse sequences could be used to quantify the T_2 values within the plaque, including the 2D multi-echo spin echo (MESE),[12,15] 2D multi-echo fast-spin-echo (MEFSE), 3D fast-spin-echo (FSE)[16] and 3D fast spoiled gradient echo (FSPGR).[11] Different black-blood techniques could be used in combination with the acquisition: double inversion-recovery (DIR),[9] motion-sensitized driven-equilibrium (MSDE)[16,17] and delay alternating with nutation for tailored excitation (DANTE).[18]

The *in vivo* quantitative T_2 measurement could be influenced by many factors, including B_0 and B_1 field inhomogeneity, stimulated echoes, T_1 effects, choice of fitting methods[19] and black-blood pulses. Some of these factors have been discussed in the previous studies.[9,19–21] With the emergence of T_2 mapping sequences for vessel wall imaging, the choice of the sequence is another factor that could influence T_2 measurement accuracy. However, there is a sparsity of comparative studies comparing *in vivo* T_2 mapping sequences.

The purpose of this work is to compare four different black-blood prepared quantitative T_2 sequences. Phantom experiments were performed comparing each respective method to the gold-standard sequence. *In vivo* volunteer experiments were then performed to enable comparison of vessel wall relaxivity values, repeatability and image quality.

Materials and Methods

Sequences

Four black-blood T_2 mapping sequences were developed and tested, including 1) DIR prepared 2D MESE; 2) DIR prepared 2D MEFSE; 3) improved motion-sensitized driven-equilibrium (iMSDE) prepared 3D FSE with variable flip angle; and 4) iMSDE prepared 3D FSPGR.

In the 3D FSE/FSPGR sequences, different echo times were achieved by varying the radio-frequency (RF) and gradient pulse intervals in the iMSDE preparation, while keeping the readout the same for different echoes. To achieve adequate blood suppression, the first moment of iMSDE preparation of the first echo in 3D FSE and FSPGR was 838.0 and 6666.7 $mTms^2/m$, respectively. The applied first moments were a result of empirical observations to achieve appropriate blood suppression for each sequence. The 3D FSE flip angle train was designed according to the vessel wall MR properties, $T_1 = 1000$ ms, $T_2 = 50$ ms, from the literature.[10] A segmented multi-shot radial fan-beam trajectory was used for 3D acquisitions.[22] The FSE-based 2D and 3D sequences acquired the different echoes using an interleaved acquisition order, while the 3D FSPGR sequence acquired the echoes sequentially. In the FSPGR sequence, 200 dummy pulses were used at the beginning of the sequence to allow the magnetization to achieve a steady state, and 50 dummy pulses were used after the acquisition to allow the magnetization recovery to reach an equilibrium state.[11] A delay time of 400 ms was used at the end of each segment for higher signal-to-noise (SNR).[23,24] The time duration for each segment was about 1200 ms. Fat saturation in the 3D FSE sequence was achieved by using an Adiabatic SPectral Inversion Recovery (ASPIR) pulse, the other three sequences used a standard chemical shift selective saturation pulse. Other imaging parameters are listed in Table 1.

Bloch simulations were performed to evaluate the vessel wall signal evolutions for the four sequences, using $T_1 = 1000$ ms and $T_2 = 50$ ms.[10]

Phantom and subjects

The four sequences were tested using the Eurospin test object gel phantoms (TO5; Diagnostic Sonar, Livingston, Scotland) with known T_2 values ranging from 52 to 136 ms at 19ºC. A 2D MESE sequence without blood suppression was used as the gold standard.

A total of 17 healthy volunteers (11 men, mean age 33, range: 23–44 years) were recruited into this study. The volunteer experiments were conducted under a research ethics agreement and all volunteers gave informed written consent. For the 2D sequences, a single axial slice 3 mm below the carotid bifurcation was chosen. For the 3D sequences, an axial slab was centered at the bifurcation. The slice thickness for all four sequences was set to 1.4 mm. To assess the repeatability, eight volunteers were scanned for the second time. The average interval between the two scans was 43 days (range 28–69 days). All the phantom and volunteer scans were performed on a 3T system (Discovery MR750 3.0T; GE Healthcare, Waukesha, WI, USA), using a 4-channel phased-array neck coil (PACC; MachNet, Roden, The Netherlands).

Image analysis and T_2 quantification

Contours of the carotid vessel wall and lumen at matched slices in the four sequences were manually drawn by a single observer who has more than 3 years of carotid imaging experience using a Digital Imaging and COmmunications in Medicine (DICOM) viewer (OsiriX 5.5.2; Pixmeo, Geneva, Switzerland). A region of noise was also drawn in an artifact-free background by the same observer. The mean value was used as the noise level.

T_2 fitting was performed by considering the noise floor in the power images using the algorithm described by Miller et al.,[25] which has previously been demonstrated to yield accurate T_2 values:[16]

$$I_c(TE)^2 = I_s(TE)^2 - I_n(TE)^2 \quad (1)$$

Table 1 Scanning parameters of the sequences for both phantom and volunteers

Sequence	2D MESE (reference)	2D MESE	2D MEFSE	3D FSE	3D FSPGR
Blood suppression	–	DIR	DIR	iMSDE	iMSDE
Number of echoes	8	8	8	3	3
Acquisition order	Interleaved	Interleaved	Interleaved	Interleaved	Sequential
Echo time (ms)	12.4–99.1 with 12.4 interval	12.9–103.2 with 12.9 interval	6.7–193.7 with 26.7 interval	25.8/55.8/85.8 (include prep)	23.2/43.2/63.2 (include prep)
Number of averages	0.5	0.5	1	1	1
Repetition time (ms)	2000	Two R-R intervals	Two R-R intervals	2000	7.1
ETL/VPS per echo	1	1	4	40	50
Bandwidth (kHz)	31.3	31.3	31.3	31.3	31.3
In-plane FOV (mm × mm)	140 × 140	140 × 140	140 × 140	140 × 140	140 × 140
Slice thickness (mm)	1.4	1.4	1.4	1.4	1.4
Matrix	224 × 224	224 × 224	224 × 224	224 × 224 × 30	224 × 224 × 30
Acquisition time	4:10	~3:03	~1:27	8:55	7:54

DIR, double inversion-recovery; ETL, echo train length; FSE, fast-spin-echo; FSPGR, fast spoiled gradient echo; iMSDE, improved motion sensitive driven equilibrium; MEFSE, multi-echo FSE; MESE, multi-echo spin echo; VPS, views per segment.

where $I_s(TE)$ and $I_n(TE)$ are the signal and background noise intensity, and $I_c(TE)$ is the corrected signal intensity at each echo. The T_2 map was then generated on a voxelwise basis by fitting the following equation to the images with different TEs using the Levenberg–Marquardt nonlinear least-squares algorithm:

$$I_c(TE)^2 = I_0^2 e^{-2TE/T_2} \quad (2)$$

where I_0^2 is the estimated power signal at $TE = 0$.

In the 2D MESE/MEFSE sequences, the first echo images were discarded due to imperfections of the 180° refocusing pulses.[9] In the 3D FSPGR sequence, sequentially acquired images were first co-registered to the first echo before performing the fitting, using a standard intensity-based registration function (*imregister* from Matlab's Image Processing Toolbox; MathWorks, Natick, MA, USA).

The mean and standard deviation of the measured T_2 values, SNR, $SNR_{efficiency}$ from the first analysed echo, and the coefficient of variance (CoV) in the carotid vessel wall from all four sequences were compared. The SNR was defined as the mean wall signal divided by the standard deviation of the background noise, and considered the four-channel coil correction[26,27]

$$SNR = 0.659 \times \frac{\text{mean wall signal}}{\text{standard deviation of noise}} \quad (3)$$

The $SNR_{efficiency}$ was defined as:

$$SNR_{efficiency} = \frac{SNR}{\sqrt{\text{acquisition time per echo}}} \quad (4)$$

The CoV was defined as following within each of the vessels:

$$CoV = \frac{\text{standard deviation of wall signal}}{\text{mean wall signal}} \quad (5)$$

Statistical analysis

For the phantom scans, the concordance correlation coefficient (CCC) and Bland–Altman summary statistics were used to compare the four sequences against the gold-standard method. For the volunteer scans, one-way analysises of variance (ANOVAs) were used to evaluate if there were gross differences between the four sequences. Paired two-tailed Student's *t*-tests were used to compare the results for parametric distributions and the Wilcoxon signed-rank test were used for non-parametric distributions. The intra-class correlation coefficient (ICC) was used to evaluate the agreement between the two repeated scans. Statistical significance was defined as a P-value < 0.05. The statistical analysis was performed using software R version 3.2.2 (R Foundation for Statistical Computing, Vienna, Austria).[28]

Results

In the phantom scans, the correlations for 2D MESE, 2D MEFSE, 3D FSE and FSPGR were all very high: $r = 0.999$, 0.999, 0.995 and 0.985, respectively, compared with the gold-standard sequence (MESE without blood suppression). The results of the Bland–Altman analysis for the four sequences compared to the reference sequence was shown in Table 2. The four sequences did not have significant bias in the phantom scans.

All the volunteers completed the MRI scans. The images from the four sequences have no apparent motion artifact. In total 34 carotid arteries were analyzed. Example images from a volunteer and the resultant T_2 maps derived using the four black-blood sequences are shown in Fig.1. The mean T_2, SNR, $SNR_{efficiency}$, CoV and their differences of the volunteer vessel walls are summarized in Table 3. One-way ANOVA demonstrates that there were significant differences between the four T_2 mapping sequences (all P-values < 0.01). In the detailed pair-wise analysis, the 2D MEFSE yielded significantly higher T_2 values than the other three sequences (52.9 ± 8.6 ms, $P < 0.05$), while T_2 measurements from 2D MESE and 3D FSE/FSPGR showed no significant difference (43.5 ± 8.2, 36.0 ± 6.5 and 41.1 ± 9.3 ms, respectively, $P > 0.05$). The highest SNR was found in the 3D FSE sequence (25.0 ± 8.8, $P < 0.05$), while the 2D MEFSE had the lowest SNR (10.8 ± 3.9). The 3D FSE also had the highest $SNR_{efficiency}$ (14.6 ± 5.1 $min^{-1/2}$, $P < 0.05$), while the other three sequences had similar $SNR_{efficiency}$ ($P > 0.05$). The CoV for the 2D

Table 2 Bland-Altman analysis of the four sequences compared to the reference sequence (MESE without blood suppresion) in the phantom

Sequence	Bias (ms)	95% CI
DIR 2D MESE	–5.9	–11.0–1.0
DIR 2D MEFSE	7.7	4.7–11
iMSDE 3D FSE	4.3	–1.5–10.0
iMSDE 3D FSPGR	2.9	–13.0–19.0

MESE, multi-echo spin echo; FSE, fast-spin-echo; MEFSE, multi-echo FSE; FSPGR, fast spoiled gradient echo; DIR, double inversion-recovery; iMSDE, improved motion sensitive driven equilibrium CI, confidence interval.

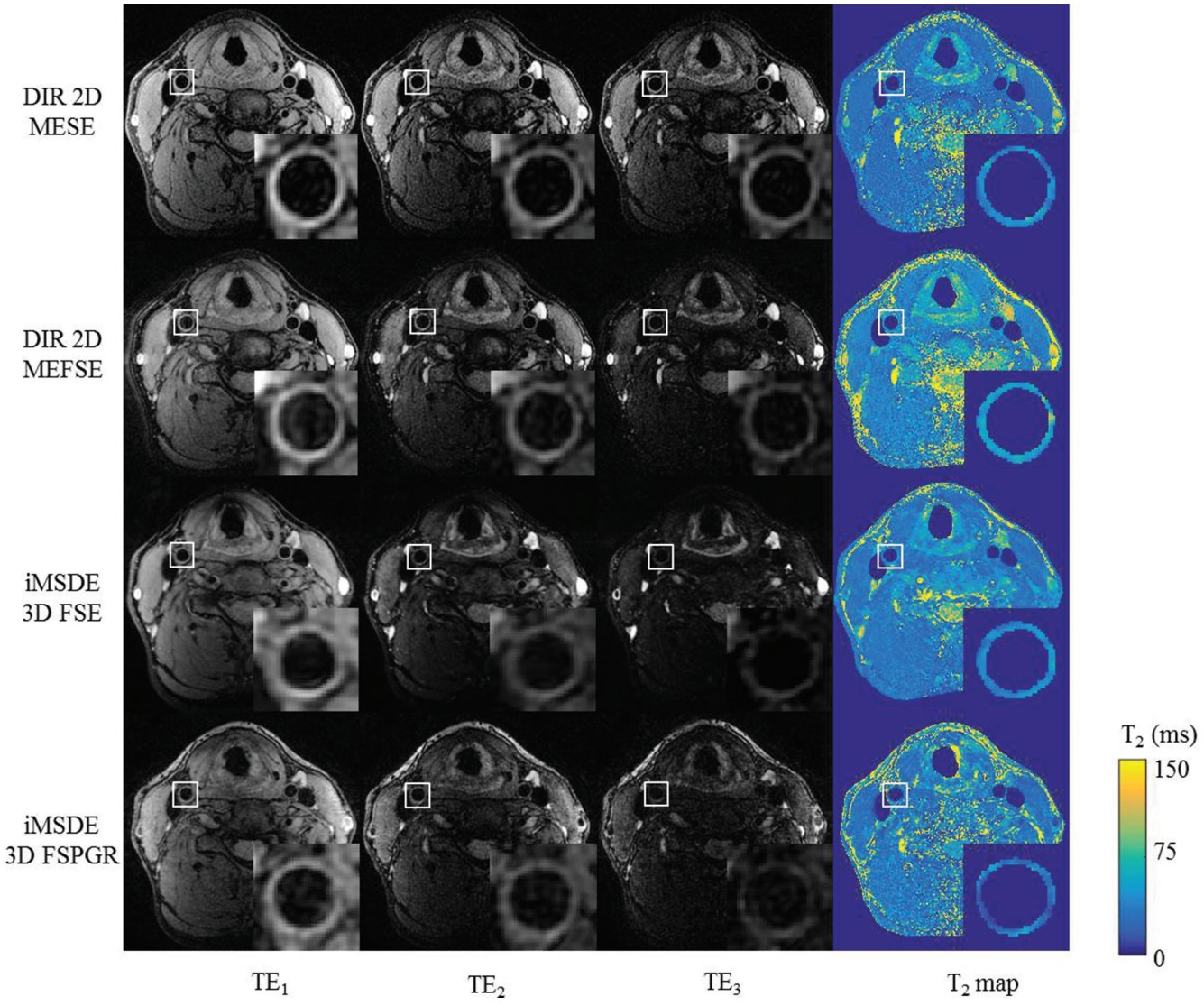

Fig. 1 An example of volunteer image and T_2 map at four different sequences. $TE_{1,2,3}$ are the first, second and third echo used for analysis. DIR, double inversion-recovery; MESE, multi-echo spin-echo; FSE, fast-spin-echo; MEFSE, multi-echo FSE; iMSDE, improved motion-sensitized driven-equilibrium; FSPGR, fast spoiled gradient echo.

MESE, 2D MEFSE and 3D FSE was similar (median and interquartile range: 40% [32–45%], 29% [24–44%] and 35% [32–42%], respectively, $P > 0.05$), but they were significantly lower compared to 3D FSPGR sequence (66% [54–75%], $P < 0.01$). The ICCs with 95% confidence interval (CI) for the repeated scans of the four sequences were: 2D MESE: 0.96 (0.88–0.99); 2D MEFSE: 0.82 (0.54–0.93); 3D FSE: 0.86 (0.63–0.95); 3D FSPGR: 0.65 (0.20–0.88).

Discussion

This study, for the first time, compared the accuracy of different black-blood T_2 mapping sequences in the carotid vessel wall. All four sequences demonstrated accurate T_2 quantifications in the phantom scans; however, it is noted that there are significant differences in the *in vivo* results as well as differences in image quality. Though all the *in vivo* T_2 measurements are comparable with previous studies.[9,11,16]

The choice of black-blood technique is an important factor for accurate T_2 measurement *in vivo*. As the irregular plaque surface and carotid bifurcation could form complex flow patterns, poor suppression of the blood flow could result in errors in vessel wall T_2 quantification, due to partial volume. In these cases, the 3D techniques showed better blood suppression compared to the 2D methods such as DIR.[24,26] The changing preparation time used in the iMSDE could potentially result in a magnetization transfer (MT) effect.[29,30] However, the iMSDE prepared 3D sequences demonstrated accurate T_2 measurements in the phantom, and comparable T_2 measurements in the volunteers with the 2D DIR MESE sequence, indicating that MT is not influencing the T_2 quantification.

The acquisition method is another consideration for vessel wall imaging. In the current study, both FSE and gradient echo (GRE)-based acquisitions were evaluated. The results showed that the 3D FSE sequence achieves a higher SNR, $SNR_{efficiency}$ and lower T_2 CoV compared to the 3D FSPGR sequence. This could be explained by the following reasons: Firstly, FSE-based readouts utilize refocusing pulses which are less sensitive to B_1^+ field non-uniformity and resonant frequency errors than GRE-based readouts. Secondly, during the FSE readout, the movement of blood spins could induce intra-voxel dephasing which results in intrinsically black-blood effects, as previously reported in other studies.[31,32] Consequently, the FSE-based sequences can use less or no black-blood preparation[33] compared to the strong blood suppression used in GRE readout, and are therefore less influenced by black-blood preparation as shown in our study.

Both 2D and 3D methods were included in this study. The use of 3D acquisitions has several advantages over 2D methods. Firstly, it allows greater longitudinal coverage. This could help with plaques located in the proximal common carotid artery or distal internal carotid artery[34] which might be missed by the more limited coverage using 2D acquisitions. Secondly, it could allow thinner slice thickness which results in less partial volume effects and potentially more accurate plaque morphological measurements.[35] Thirdly, 3D readouts can achieve more rectangular slice profiles compared to 2D sequences, which should result in more accurate T_2 measurement. Though setting the slice thickness of refocusing pulse larger than the excitation pulse can also minimize this effect.[15] Fourthly, the 3D sequences have higher SNR as our results showed. However, this also leads to one of the disadvantages of the 3D methods. Since the signals are from the entire imaging volume, any movement during the acquisition could influence the entire dataset, so the 3D methods are potentially more prone to motion artifact. However, the volunteer images in this study showed no obvious motion artifact.

For the 2D sequences, the MEFSE demonstrated significantly higher T_2 values than MESE in volunteers, as shown in Table 3. Similar results were reported in previous studies.[20,21] Imperfections in the 180° refocusing pulses cause stimulated echoes which lead to higher signal intensities in later echoes.[19,36] This phenomenon is more obvious in 2D FSE sequences with longer echo train lengths.[21]

The optimal sequence in this study, iMSDE 3D FSE, has the advantages for both non-selective blood suppression and 3D readout as discussed above. The volunteer scans in this study demonstrate sufficient blood suppression and high image quality. Any slight patient motion is effectively

Table 3 Mean and SD of averaged vessel wall T_2 measurement

	DIR 2D MESE	DIR 2D MEFSE	iMSDE 3D FSE	iMSDE 3D FSPGR	*P*-value
$T_2 \pm$ SD (ms)	43.5 ± 8.2	52.9 ± 8.6*	36.0 ± 6.5	41.1 ± 9.3	<0.01
SNR ± SD	11.1 ± 2.6	10.8 ± 3.9	25.0 ± 8.8*	13.8 ± 7.4	<0.01
$SNR_{efficiency} \pm$ SD ($min^{-1/2}$)	6.3 ± 1.5	9.0 ± 3.3	14.6 ± 5.1*	8.6 ± 4.6	<0.01
CoV (median with IQR, %)	40 (32–45)	29 (24–44)	35 (32–42)	66 (54–75)*	<0.01

Signal-to-noise ratio (SNR), $SNR_{efficiency}$ and coefficient of variance (CoV) derived from four sequences, and their one-way analysis of variance (ANOVA) differences (*P*-values) in the volunteer scans. Paired two-tailed Student's *t*-test result is also showing in the table. *Stands for significantly higher value ($P < 0.05$) compared with any one of the other three sequences. DIR, double inversion-recovery; FSE, fast-spin-echo; FSPGR, fast spoiled gradient echo; iMSDE, improved motion sensitive driven equilibrium; IQR, Interquartile range; MEFSE, multi-echo FSE; SD, standard deviation.

averaged by acquiring 3D data. Nevertheless, future developments could include the use of acceleration techniques, such as compressed sensing and parallel imaging, SNR permitting to reduce the acquisition time,[16] and include the use of an immobilization device such as a vacuum-based pillow to reduce the potential for subject movement.[37]

The T_2 calculation based on Miller's method[25] was used in this study. There are other curve fitting methods used in the literature, such as two-parameter fitting without noise correction[9,12] or three-parameter fitting method.[38] Miller's power correction was applied in this study as the 3D sequences only acquired three echoes. This approach prevented the noise floor contributing to errors in T_2 calculations.[39]

There are four main limitations in this study. Firstly, the three FSE-based sequences acquired multiple echoes in an interleaved manner, while the FSPGR sequence acquired the echoes sequentially, which was the same method used in a previous study.[11] Hence, image registration was needed for the 3D FSPGR sequence, which may potentially introduce further errors into the T_2 analysis. However, in this study, no obvious motion was observed in the volunteer data, but it may be difficult for patients to keep still giving such a long acquisition time. Thus, an interleaved acquisition may be preferable, further time reduction strategies such as parallel imaging[40] and compressed sensing,[16,23,41] should be investigated. Secondly, these methods were only evaluated in normal volunteers. However, the optimal sequence from this study is worth applying to the patient studies. Thirdly, the gold-standard sequence, 2D MESE without blood suppression, was only used in the phantom, not in the volunteer scan. The sequence is not particularly useful for imaging the carotid artery wall *in vivo* due to flow artifact from the pulsatile blood flow and relative long scan time. The phantom results showed excellent agreement between the gold standard and all other sequences; therefore, we did not consider it necessary to try and obtain *in vivo* results using this sequence. The results in this study showed vessel wall T_2 values measured by the sequences (except DIR 2D MEFSE) are in agreement with other studies.[11,16] Fourthly, for both phantom and volunteer studies, the effect of T_1 was not considered. However, from the phantom scans, accurate T_2 measurement can be achieved with different test tube. Future validation should consider the influence of T_1 in the T_2 measurement for more precise quantification.

Conclusion

Four different black-blood T_2 mapping sequences were developed and validated through phantom experiments and in a cohort of healthy volunteers. Although the phantom scans showed accurate T_2 measurement, the *in vivo* measurements of the four sequences were significantly different. Therefore, a careful choice of T_2 mapping sequence is warranted for carotid vessel wall imaging. From the settings in this study, the iMSDE prepared 3D FSE is preferred for the future volunteer/patient scans.

Acknowledgments

The project was supported by the Addenbrooke's Charitable Trust and the NIHR comprehensive Biomedical Research Centre award to Cambridge University Hospitals NHS Foundation Trust in partnership with the University of Cambridge. We thank Dr. Roido Manavaki for insightful discussions.

Conflicts of Interest

Scott A. Reid is an employee of GE Healthcare. The other authors have no conflicts of interest.

References

1. Truelsen T, Piechowski-Jóźwiak B, Bonita R, et al. Stroke incidence and prevalence in Europe: a review of available data. Eur J Neurol 2006; 13:581–598.
2. Hoyert DL, Xu J. Deaths: preliminary data for 2011. Natl Vital Stat Rep 2012; 61:1–51.
3. Saam T, Ferguson MS, Yarnykh VL, et al. Quantitative evaluation of carotid plaque composition by in vivo MRI. Arterioscler Thromb Vasc Biol 2005; 25:234–239.
4. Yuan C, Mitsumori LM, Ferguson MS, et al. In vivo accuracy of multispectral magnetic resonance imaging for identifying lipid-rich necrotic cores and intraplaque hemorrhage in advanced human carotid plaques. Circulation 2001; 104:2051–2056.
5. Kerwin WS. Carotid artery disease and stroke: assessing risk with vessel wall MRI. ISRN Cardiol 2012; 2012:180710. doi: 10.5402/2012/180710.
6. Yuan J, Usman A, Das T, Patterson AJ, Gillard JH, Graves MJ. Imaging carotid atherosclerosis plaque ulceration: comparison of advanced imaging modalities and recent developments. AJNR Am J Neuroradiol 2017; 38:664–671.
7. Yuan J, Makris G, Patterson A, et al. Relationship between carotid plaque surface morphology and perfusion: a 3D DCE-MRI study. MAGMA 2018; 31:191–199.
8. Yuan J, Usman A, Reid SA, et al. Three-dimensional black-blood multi-contrast carotid imaging using compressed sensing: a repeatability study. MAGMA. 2018; 31:183-190.
9. Biasiolli L, Lindsay AC, Chai JT, Choudhury RP, Robson MD. In-vivo quantitative T2 mapping of carotid arteries in atherosclerotic patients: segmentation and T2 measurement of plaque components. J Cardiovasc Magn Reson 2013; 15:69.
10. Degnan AJ, Young VE, Tang TY, et al. Ex vivo study of carotid endarterectomy specimens: quantitative relaxation times within atherosclerotic plaque tissues. Magn Reson Imaging 2012; 30:1017–1021.
11. Coolen BF, Poot DH, Liem MI, et al. Three-dimensional quantitative T1 and T2 mapping of the carotid artery:

Sequence design and in vivo feasibility. Magn Reson Med 2016; 75:1008–1017.
12. Proniewski B, Miszalski-Jamka T, Jaźwiec P. In vivo T2-mapping and segmentation of carotid artery plaque components using magnetic resonance imaging at 1.5 T. Computing in Cardiology Conference Massachusetts, USA. CinC 2014; 41:921–924.
13. Chai JT, Biasiolli L, Li L, et al. Quantification of lipid-rich core in carotid atherosclerosis using magnetic resonance t2 mapping: relation to clinical presentation. JACC Cardiovasc Imaging 2017; 10:747–756.
14. Yuan J, Graves MJ, Patterson AJ, et al. The development and optimisation of 3D black-blood R2* mapping of the carotid artery wall. Magn Reson Imaging 2017; 44:104–110.
15. Biasiolli L, Chai JT, Li L, et al. Histological validation of carotid plaque characterization by in-vivo T2 mapping in patients with recent cerebrovascular events: preliminary results. J Cardiovasc Magn Reson 2014; 16:1.
16. Yuan J, Usman A, Reid SA, et al. Three-dimensional black-blood T2 mapping with compressed sensing and data-driven parallel imaging in the carotid artery. Magn Reson Imaging 2017; 37:62–69.
17. Wang J, Yarnykh VL, Yuan C. Enhanced image quality in black-blood MRI using the improved motion-sensitized driven-equilibrium (iMSDE) sequence. J Magn Reson Imaging 2010; 31:1256–1263.
18. Li L, Miller KL, Jezzard P. DANTE-prepared pulse trains: a novel approach to motion-sensitized and motion-suppressed quantitative magnetic resonance imaging. Magn Reson Med 2012; 68:1423–1438.
19. Poon CS, Henkelman RM. Practical T2 quantitation for clinical applications. J Magn Reson Imaging 1992; 2:541–553.
20. Maier CF, Tan SG, Hariharan H, Potter HG. T2 quantitation of articular cartilage at 1.5 T. J Magn Reson Imaging 2003; 17:358–364.
21. Pai A, Li X, Majumdar S. A comparative study at 3 T of sequence dependence of T2 quantitation in the knee. Magn Reson Imaging 2008; 26:1215–1220.
22. Vu AT. Method and apparatus for acquiring MR data with a segmented multi-shot radial fan beam encoding order. Google Patents; 2007. US7265547B2. September 4
23. Li B, Li H, Li J, et al. Relaxation enhanced compressed sensing three-dimensional black-blood vessel wall MR imaging: Preliminary studies. Magn Reson Imaging 2015; 33:932–938.
24. Li L, Chai JT, Biasiolli L, et al. Black-blood multicontrast imaging of carotid arteries with DANTE-prepared 2D and 3D MR imaging. Radiology 2014; 273:560–569.
25. Miller AJ, Joseph PM. The use of power images to perform quantitative analysis on low SNR MR images. Magn Reson Imaging 1993; 11:1051–1056.
26. Ducas RA, Elliott JE, Melnyk SF, et al. Cardiovascular magnetic resonance in pregnancy: insights from the cardiac hemodynamic imaging and remodeling in pregnancy (CHIRP) study. J Cardiovasc Magn Reson 2014; 16:1.
27. Constantinides CD, Atalar E, McVeigh ER. Signal-to-noise measurements in magnitude images from NMR phased arrays. Magn Reson Med 1997; 38:852–857.
28. R Development Core Team. R: A language and environment for statistical computing. Vienna, Austria: the R Foundation for Statistical Computing; 2013. http://www.R-project.org/. (Accessed August 14, 2015).
29. Yarnykh VL, Yuan C. T1-insensitive flow suppression using quadruple inversion-recovery. Magn Reson Med 2002; 48:899–905.
30. Hu BS, Conolly SM, Wright GA, Nishimura DG, Macovski A. Pulsed saturation transfer contrast. Magn Reson Med 1992; 26:231–240.
31. Alexander AL, Buswell HR, Sun Y, Chapman BE, Tsuruda JS, Parker DL. Intracranial black-blood MR angiography with high-resolution 3D fast spin echo. Magn Reson Med 1998; 40:298–310.
32. Jara H, Yu BC, Caruthers SD, Melhem ER, Yucel EK. Voxel sensitivity function description of flow-induced signal loss in MR imaging: implications for black-blood MR angiography with turbo spin-echo sequences. Magn Reson Med 1999; 41:575–590.
33. Smit H, Leeuw HD, Guridi RP, et al. T2 mapping in the carotid artery with T2 prepared signal stabilized 3D fast spin echo. European Society for Magnetic Resonance in Medicine and Biology, Toulouse, 2013; 217.
34. Zhao X, Balu N, Wang J, Zhao H, Xu J, Yuan C. Carotid atherosclerotic lesion distribution in patients with cerebrovascular events: a 3.0 tesla magnetic resonance vessel wall imaging study using three-dimensional, isotropic, fast sequence with large coverage. Proceedings of the Annual Meeting of ISMRM, Montréal, 2011; 467.
35. Balu N, Chu B, Hatsukami TS, Yuan C, Yarnykh VL. Comparison between 2D and 3D high-resolution black-blood techniques for carotid artery wall imaging in clinically significant atherosclerosis. J Magn Reson Imaging 2008; 27:918–924.
36. Majumdar S, Orphanoudakis SC, Gmitro A, O'Donnell M, Gore JC. Errors in the measurements of T2 using multiple-echo MRI techniques. I. Effects of radiofrequency pulse imperfections. Magn Reson Med 1986; 3:397–417.
37. Young VE, Patterson AJ, Tunnicliffe EM, et al. Signal-to-noise ratio increase in carotid atheroma MRI: a comparison of 1.5 and 3 T. Br J Radiol 2012; 85:937–944.
38. Krishnamurthy R, Pednekar A, Atweh LA, et al. Clinical validation of free breathing respiratory triggered retrospectively cardiac gated cine balanced steady-state free precession cardiovascular magnetic resonance in sedated children. J Cardiovasc Magn Reson 2015; 17:1.
39. Chen X, Zhang H, Yang Q, et al. Value of severe liver iron overload for assessing heart iron levels in thalassemia major patients. J Magn Reson Imaging 2016; 44:880–889.
40. Johansson B, Babu-Narayan SV, Kilner PJ. The effects of breath-holding on pulmonary regurgitation measured by cardiovascular magnetic resonance velocity mapping. J Cardiovasc Magn Reson 2009; 11:1.
41. Li B, Dong L, Chen B, et al. Turbo fast three-dimensional carotid artery black-blood MRI by combining three-dimensional MERGE sequence with compressed sensing. Magn Reson Med 2013; 70:1347–1352.